Synthesis, Characterization, Properties, and Drug Release of Poly(alkyl methacrylate-*b*-isobutylene-*b*-alkyl methacrylate)

Jae Cheol Cho, Guanglou Cheng, Dingsong Feng, and Rudolf Faust*

Department of Chemistry, University of Massachusetts Lowell, One University Avenue, Lowell, Massachusetts 01854

Robert Richard, Marlene Schwarz, Ken Chan, and Mark Boden*

Corporate Research & Advanced Technology, Boston Scientific Corporation, One Boston Scientific Place, Natick, Massachusetts 01760

Received May 8, 2006; Revised Manuscript Received July 27, 2006

Polyisobutylene (PIB)-based block copolymers have attracted significant interest as biomaterials. Poly(styrene-*b*-isobutylene-*b*-styrene) (SIBS) has been shown to be vascularly compatible and, when loaded with paclitaxel (PTx) and coated on a coronary stent, has the ability to deliver the drug directly to arterial walls. Modulation of drug release from this polymer has been achieved by varying the drug/polymer ratio, by blending SIBS with other polymers, and by derivatizing the styrene end blocks to vary the hydrophilicity of the copolymer. In this paper, results are reported on the synthesis, physical properties, and drug elution profile of PIB-based block copolymers containing methacrylate end blocks. The preparation of PIB−poly(alkyl methacrylate) block copolymers has been accomplished by a new synthetic methodology using living cationic and anionic polymerization techniques. 1,1-Diphenylethylene end-functionalized PIB was prepared from the reaction of living PIB and 1,4-bis(1-phenylethenyl)benzene, followed by the methylation of the resulting diphenyl carbenium ion with dimethylzinc ($Zn(CH_3)_2$). PIB-DPE was quantitatively metalated with *n*-butyllithium in tetrahydrofuran, and the resulting macroinitiator could initiate the polymerization of methacrylate monomers, yielding block copolymers with high blocking efficiency. Poly(methyl methacrylate-*b*-isobutylene-*b*-methyl methacrylate) (PMMA-*b*-PIB-*b*-PMMA) and poly(hydroxyethyl methacrylate-*b*-isobutylene-*b*-hydroxyethyl methacrylate) (PHEMA-*b*-PIB-*b*-PHEMA) triblock copolymers were synthesized and used as drug delivery matrixes for coatings on coronary stents. The PMMA-*b*-PIB-*b*-PMMA/PTx system displayed zero-order drug release, while stents coated with PHEMA-*b*-PIB-*b*-PHEMA/PTx formulations exhibited a significant initial burst release of PTx. Physical characterization using atomic force microscopy and differential scanning calorimetry of the formulated PMMA-*b*-PIB-*b*-PMMA coating matrix indicated the partial miscibility of PTx with the PMMA microphase of the matrix.

Introduction

Poly(styrene-*b*-isobutylene-*b*-styrene) (SIBS) triblock copolymers are used as drug eluting coatings for the TAXUS stent. These stents are used in the coronary vasculature to dilate the arteries and to provide a scaffold to maintain patency. The introduction of a paclitaxel (PTx) containing stent coating that delivers the drug directly to the vessel wall has been shown to greatly reduce restenosis rates in several controlled clinical trials.[1−7] The coatings must be biocompatible, sterilizable, be able to withstand handling during the manufacturing process and general use, and expand in the vasculature while maintaining structural integrity as they are passed through complex lesions. ABA triblock copolymers consisting of rubbery mid-blocks and glassy or crystalline end-blocks exhibit properties that make them uniquely suited for application as a stent coating and drug delivery matrix.[8−10] In the case of the SIBS copolymers, the rubbery mid-block imparts excellent adhesion and elongation to the coating, while the hard segments provide physical strength. Since the copolymers are not chemically cross-linked, they can be processed from solution with no post-coating cure step. They can be sterilized by ethylene oxide without changes in the physical or chemical properties and have proven biocompatibility and noninflammatory properties.[11]

The SIBS polymer is relatively hydrophobic, with both the backbone and side pendant groups containing only carbon−carbon and carbon−hydrogen bonds. Since PTx contains both hydrophobic and hydrophilic portions, the drug is incompatible with SIBS. The polymer and drug separate into separate domains, and PTx diffusion through SIBS is extremely slow. Recently, it was shown that the hydrophilic nature of the end blocks and the polarity effects on the drug−polymer miscibility in a poly(hydroxystyrene-*b*-isobutylene-*b*-hydroxystyrene)/PTx system allows flexibility in tuning the drug release rate.[10] Both differential scanning calorimetry (DSC) and atomic force microscopy (AFM) data support the conclusion that the drug is at least partially miscible with the more polar poly(hydroxy styrene) end blocks.

Isobutylene (IB) can be polymerized only by cationic methods. However, many polar monomers, for example, methacrylates, do not undergo cationic polymerization. Recently, there has been much interest in the synthesis of block copolymers using two different living polymerization methods. The combination of various polymerization techniques provides a unique approach to block copolymers not available by a single method. Since relatively few monomers can be polymerized by cationic or anionic polymerization compared with other living polymerization methods, there have been many efforts to combine cationic and anionic polymerization. Block copolymers

* Corresponding author.

10.1021/bm0604496 CCC: $33.50
Published on Web 10/27/2006

of IB and polar monomers, such as acrylates and methacrylates, combine the biocompatibility and the thermal, oxidative, and biostability of elastomeric, nonpolar polyisobutylene (PIB) with a variety of properties of polar polymers.

Methacrylate-based polymers such as poly(methyl methacrylate) (PMMA) and poly(hydroxyethyl methacrylate) (PHEMA) have a significant history and track record of safety in implantable medical device applications. PMMA is a key component of the bone cement used in artificial knee and hip implants,[12] and PHEMA has been used extensively in contact lens applications.[13] Therefore, triblock copolymers based on these polymers have been considered outstanding candidates for polymer matrixes for the application of drug-eluting stent coatings.

Since PIB can only be obtained by carbocationic polymerization, many attempts have been reported to transform living PIB to a macroinitiator for anionic polymerization. Recently, Mueller et al. reported that polyisobutylene-*b*-polymethacrylate (PIB-*b*-PMA) block copolymers could be prepared by the combination of cationic and anionic polymerizations.[14,15] First, 1,1-diphenyl-1-methoxy or 2,2-diphenylvinyl end-functionalized PIB was prepared by the reaction of 1,1-diphenylethylene (DPE) and living PIB. The chain end of DPE-end-capped PIB was metalated with alkali metals, in tetrahydrofuran (THF) at room temperature, and the resulting macroanion obtained by metalation with a K/Na alloy was used to initiate the living anionic polymerization of *tert*-butyl methacrylate (*t*BMA), yielding PIB-*b*-P*t*BMA block copolymers. A series of linear PMMA-*b*-PIB-*b*-PMMA block copolymers and star-shaped PIB-*b*-$(PMMA)_3$ block copolymers were also successfully synthesized by replacing K^+ with Li^+ by using excess LiCl. The linear triblock copolymers, however, exhibited rather poor mechanical properties, suggesting diblock contamination. Metalation using alkali metal compounds is also inconvenient, and lithiation with alkyllithium would be preferable. However, the lithiation of 2,2-diphenylvinyl-end-functionalized PIB with alkyllithium does not proceed quantitatively.[16] An improved method for the cationic−anionic transformation, reported recently,[17] involves the preparation of 2-polyisobutenyl-thiophene in a simple addition reaction of thiophene and living PIB, followed by metalation of the thiophene end using *n*-butyllithium (*n*-BuLi). The resulting stable macrocarbanion was used to initiate the living anionic polymerization of *t*BMA, yielding PIB-*b*-P*t*BMA block copolymers with high (about 80%) blocking efficiency.[17]

We recently reported that DPE-end-functionalized PIB (PIB-DPE) could be prepared by the monoaddition reaction of 1,3-bis(1-phenylethenyl)benzene (*meta*-double DPE, MDDPE) or 1,4-bis(1-phenylethenyl)benzene (*para*-double DPE, PDDPE) and living PIB.[18,19] It was found that the use of PDDPE for the preparation of PIB-DPE is more advantageous than using MDDPE because the coupling reaction was absent, and functionalization was ~100%.

In this study, we report a new methodology to prepare block copolymers comprised of PIB and PMMA or PHEMA by using PIB-DPE. The PIB-DPE macromonomer can be easily and efficiently metalated with alkyllithium compounds, and the resulting diphenyl carbanion is an efficient initiator for the polymerization of methacrylates.

We also report on the miscibility of PTx with the acrylate end blocks and the effect of the nature of the end blocks on diffusion and drug release from stent coatings.

Experimental Section

Materials. 2-Chloro-2,4,4-trimethylpentane (TMPCl) and 5-*tert*-butyl-1,3-bis(1-chloro-1-methylethyl)benzene (*t*BuDiCumCl) were synthesized following the procedures reported elsewhere.[20,21] PDDPE was prepared by using procedures analogous to those reported by Tung and Lo.[22] 2,6-Di-*tert*-butylpyridine (DTBP, Aldrich, 97%), titanium tetrachloride ($TiCl_4$, Aldrich, 99.9%), dimethylzinc ($Zn(CH_3)_2$, Aldrich, 2.0 M in toluene), *n*-BuLi (Aldrich, 1.6 M in HX), triethylaluminum ($AlEt_3$, Aldrich, 25 wt % in toluene), and trioctylaluminum ($AlOct_3$, Aldrich, 25 wt % in HX) were used as received. DPE (Aldrich, 97%) was used without further purification. THF (Aldrich, 99+%) was distilled from CaH_2 and from Na metal sequentially and was then distilled into a flask containing Na/benzophene. Methyl methacrylate (MMA, Aldrich, 99%) was dried over CaH_2 for 24 h and then distilled into a flask containing $AlEt_3$.[23] When a yellow color persisted for several hours at room temperature, MMA was distilled into an ampule with a break-seal and then sealed off with a flame. 2-[(Trimethylsilyl)oxy]ethyl methacrylate (TMSiOEMA, Gelest, >95%) was dried over CaH_2 for 24 h and then distilled into a flask containing $AlOct_3$.[23,24] When the TMSiOEMA/$AlOct_3$ solution exhibited a yellow color, TMSiOEMA was distilled into an ampule with a break-seal. A small amount of THF was distilled into the ampule to dilute the monomer, and the ampule was sealed off with a flame. Hexanes (HX), methyl chloride (MeCl), methylene chloride (CH_2Cl_2), and IB (Airgas) were purified as described previously.[25−27]

Synthesis of *ω*-DPE-Functionalized PIB (PIB-DPE). The preparation of PIB-DPE was carried out at −80 °C under a dry nitrogen atmosphere in an MBraun 150-M glovebox. To a prechilled 500 mL three-neck flask equipped with a mechanical stirrer were added 180 mL of HX, 120 mL of MeCl, 0.1 mL of TMPCl (0.6 mmol), 0.2 mL of DTBP (0.9 mmol), and 4.7 mL of IB (60 mmol), sequentially. Then 1.18 mL of $TiCl_4$ (10.8 mmol) dissolved in HX/MeCl was added to polymerize IB. After the completion of the polymerization, 0.34 g of PDDPE (1.2 mmol) dissolved in 40 mL of CH_2Cl_2 was added into the reactor ([PDDPE]/[TMPCl] = 2/1). After 3 h, 27 mL of prechilled $Zn(CH_3)_2$ (54 mmol) was added to the reactor ($[Zn(CH_3)_2/[TiCl_4]$ = 5/1). Following the methylation, the reaction mixture was quenched with prechilled methanol and poured into a methanol/ammonium hydroxide 90/10 (v/v) solution. After the evaporation of solvent, the crude product was dissolved in HX, and the inorganic salts were removed by filtration. The polymer solution was poured into methanol to precipitate the polymer, and the solvent was decanted. The dissolution/precipitation procedure of the polymer was repeated three times to remove unreacted PDDPE. Finally, the obtained polymer was dried in a vacuum oven at 50 °C for at least 48 h.

Synthesis of α,*ω*-DPE-Functionalized PIB (DPE-PIB-DPE). DPE-PIB-DPE was prepared using *t*BuDiCumCl as an initiator for the polymerization of IB in a manner similar to that for the synthesis of PIB-DPE. To a prechilled 500 mL three-neck flask equipped with a mechanical stirrer were added 167 mL of HX and 111 mL of MeCl. Then, 0.086 g of *t*BuDiCumCl (0.3 mmol), 0.2 mL of DTBP (0.9 mmol), and 21 mL of IB (0.27 mol) were added sequentially. To polymerize IB, 1.18 mL of $TiCl_4$ (10.8 mmol) dissolved in HX/MeCl was added. After 2 h of polymerization time, 0.34 g of PDDPE (1.2 mmol) dissolved in 40 mL of methylene chloride was added into the reactor ([PDDPE]/[*t*BuDiCumCl] = 4/1). The end-capping reaction was allowed to proceed for 3 h, after which 27 mL of $Zn(CH_3)_2$ (54 mmol) was added to the reactor ($[Zn(CH_3)_2/[TiCl_4]$ = 5/1). After 2 h, the reaction mixture was quenched with prechilled methanol and poured into methanol. The MeCl was allowed to evaporate prior to the isolation of the polymer from the HX/methanol mixture solvents by decantation and then redissolving in HX. The polymer solution was washed with a 7.5% NaCl/77.5% water/15% 2-propanol solution three times and with distilled water two times. Then, the dissolution/precipitation procedure was repeated three times. Finally, the purified polymer solution was precipitated into methanol to give a clear polymer, which was dried in a vacuum oven at 50 °C for 48 h.

UV−Visible (UV−vis) Spectroscopy. In situ UV−vis spectroscopic monitoring of the PDDPE end-capping and the $ZnMe_2$ methylation reaction was carried out using a quartz immersion probe (661.300-QX, Hellma, optical path: 0.02 cm) connected to a fiber optic visible (Tungsten light source, Ocean Optics) and UV (AIS model UV-2, Analytical Instrument Systems, Inc.) light source, and a Zeiss MMS 256 photodiode array detector was used. The latter was connected to a personal computer via a TEC5 interface, and the spectra were recorded using the "Aspect Plus" software (Zeiss).

Preparation of 1,1-Diphenylhexyllithium (DPHLi). DPHLi solution was prepared according to the following representative procedure: To a 250 mL flask were added 47.5 mL of THF and 0.6 mL of *n*-BuLi (0.96 mmol) under high vacuum conditions ($<10^{-6}$ mbar). Then, at −78 °C, 0.032 g of DPE (0.18 mmol) was added to the reactor. The red-colored solution was kept at room temperature for 2 h to decompose the unreacted *n*-BuLi. The solution was stored in a refrigerator until use.

Synthesis of PIB-*b*-PMMA. All the polymerizations of MMA were carried out under high vacuum conditions ($<10^{-6}$ mbar) using break-seals and Rotaflo stopcocks. A 0.34 g portion of PIB-DPE ($M_n = 4900$, 0.07 mmol) dissolved in 200 mL of HX was stirred over CaH_2 for 24 h, and then CaH_2 was removed by filtration. After the evaporation of HX, 30 mL of THF was added to the polymer, and the polymer solution was delivered to the reactor. Then, DPHLi solution was added dropwise to the reactor at room temperature until the color of the polymer solution turned yellow, indicating that there were no protic impurities in the polymer solution. After DPHLi cleansing, two different lithiation procedures were employed to metalate PIB-DPE to form the anionic PIB macroinitiator. In the first method, the polymer solution was cooled to −78 °C and 0.22 mL of *n*-BuLi (0.35 mmol) was added into the reactor with vigorous stirring. After 1 h, the polymer solution was heated to 40 °C and kept for 1 h. Then, the polymer solution was cooled to −78 °C, and 2 mL of MMA (18.6 mmol) was distilled into the reactor. The second lithiation method, 1.5−2 times excess *n*-BuLi was added at room temperature for 5−10 min. After the completion of the polymerization of MMA at −78 °C, degassed methanol was added to the reactor to terminate the living polymer. The solution was poured into methanol to give a white solid polymer, which was dried in a vacuum oven. The polymer was stirred with HX to remove the deactivated PIB macromonomer at room temperature for 24 h.

Synthesis of PMMA-*b*-PIB-*b*-PMMA. The synthesis of the triblock copolymer was carried out using DPE-PIB-DPE in a manner similar to that of PIB-*b*-PMMA. A 6.7 g portion of DPE-PIB-DPE (M_n = 54 000, 0.12 mmol) dissolved in 300 mL of HX was stirred over CaH_2 for 24 h, and then the CaH_2 was removed by filtration. After the evaporation of HX, 170 mL of THF was added to the polymer, and the polymer solution was added to a 1 L reactor. Then, 180 mL of THF and 130 mL of HX were added into reactor. DPHLi was then added dropwise into the reactor at room temperature until the color of the polymer solution turned yellow. The polymer solution was cooled to −78 °C, and 0.42 mL of *n*-BuLi (0.67 mmol), which was diluted with 20 mL of HX, was added into the reactor with vigorous stirring. After 1 h, the polymer solution was heated to 40 °C and kept for 1 h to destroy the unreacted *n*-BuLi. Then, the polymer solution was cooled to −78 °C, and 5.0 mL of MMA (46.7 mmol) was distilled into the reactor. After 1 h polymerization time, degassed methanol was added to the reactor to quench the reaction. The polymer solution was poured into methanol, and the obtained polymer was dried in a vacuum oven. The polymer was purified by the extraction of the deactivated PIB macromer with HX.

Synthesis of PHEMA-*b*-PIB-*b*-PHEMA. The polymerization of TMSiOEMA was carried out similarly to that of MMA above using the difunctional macroinitiator from the reaction of DPE-PIB-DPE with *n*-BuLi in THF/HX 70/30 (v/v). After the polymerization of TMSiOEMA, the reaction was quenched with a few drops of methanol. The polymer solution was precipitated into HX. As the polymer solution was exposed to air and the trimethylsilyl protecting group of the P(TMSiOEMA) block was cleaved, the block copolymer did not precipitate in methanol. To characterize the PHEMA-*b*-PIB-*b*-PHEMA copolymer using gel permeation chromatography (GPC) and NMR, it was esterified with benzoic anhydride.[28]

Nuclear Magnetic Resonance ^{1}H NMR spectra were measured on a Bruker 250 or 500 MHz spectrometer using $CDCl_3$ as a solvent.

Molecular Weight Characterization. Molecular weights and molecular weight distributions of polymers were measured using a Waters high-performance liquid chromatography (HPLC) system equipped with a model 510 HPLC pump, a model 410 differential refractometer, a model 486 UV−vis detector, a model 712 sample processor, and five Waters ultraStyragel columns connected in series (500, 10^3, 10^4, 10^5, and 100 Å). THF was used as an eluent at a flow rate of 1 mL/min.

Differential Scanning Calorimetry. Films of the PMMA-*b*-PIB-*b*-PMMA and PHEMA-*b*-PIB-*b*-PHEMA copolymers blended with between 0 and 25% PTx were prepared for analysis using DSC. The glass transition temperatures (T_g) of the copolymer blends were determined by a TA Instruments Q1000 differential scanning calorimeter using a heating rate of 20 °C/min. Samples for compatibility evaluations were heated above their T_g on the first heat to provide a consistent history. They were then cooled at 20 °C/min to eliminate effects from residual solvents and variations in sample preparation. Data were collected on the second heating cycle for compatibility analysis. The results presented are the average values determined from multiple sample runs. All instruments were calibrated against indium.

Films of SIBS containing 0, 10, and 25% PTx were cast from a 5% solids solution containing 5% THF/90% toluene into a Teflon dish. The samples were dried under ambient conditions for 16 h, followed by 24 h at 65 °C under vacuum. Prior to evaluation, the test samples were cut using a 3/8 in. die punch.

Test samples of PMMA-*b*-PIB-*b*-PMMA with varying levels of PTx from 0 to 25% in 5% increments were prepared from 5% solids solutions in 95% CH_2Cl_2. Samples of PHEMA-*b*-PIB-*b*-PHEMA with 0, 10, and 25% PTx were prepared from 15% solid solutions in 85% THF. Both sets of samples were cast directly into aluminum DSC pans and dried at 40 °C with a vacuum for at least 40 h.

Mechanical Properties. The tensile properties were measured on solution-cast or compression-molded samples according to ASTM D638-02a. Solution-cast samples were prepared by dissolving the polymer in toluene (1−5 wt %). After complete dissolution, the solution was poured into a Teflon mold. The poured sample was dried slowly for ∼5 days at room temperature to avoid bubbles in the sample followed by vacuum-drying for 2 days at room temperature. Compression molding was carried out at 180 °C for 20 min (5 min under 1000 lb followed by 15 min at 9000 lb).

Scanning Electron Microscopy (SEM). Stents were coated with a drug/polymer layer by a proprietary process. The mechanical integrity of the coated stents was examined using a JEOL JSM-6460 scanning electron microscope (Tokyo, Japan). Coated stents did not require an additional coating of a conductive thin layer (e.g., gold or carbon) prior to examination. An accelerating voltage of 1 kV was used for collecting the secondary electron images.

Atomic Force Microscopy. Polymer morphologies at the stent coating surface were determined using AFM analysis. A Dimension 3100 AFM (Digital Instruments/Veeco Metrology, Santa Barbara, CA) controlled with NanoScope IV and NanoScope Extender electronics was used. Stents coated with SIBS and PMMA-*b*-PIB-*b*-PMMA polymers with and without PTx were analyzed by AFM.

Stent samples were initially examined in the dry state using the tapping mode. Subsequently, the stents were exposed to an excess of the release medium (phosphate-buffered saline (PBS)−Tween 20) at room temperature while mounted in the AFM sample holder. AFM images of the stent surface were gathered at specific time intervals as PTx was released from the coating by running with the AFM probe tip submerged in the release medium. Information regarding the release of PTx and its effect on the polymer morphology was gathered.

Because of the hydrophilic nature of the PHEMA polymer, it was

Scheme 1. Synthesis of ω-DPE-Functionalized PIB (PIB-DPE)

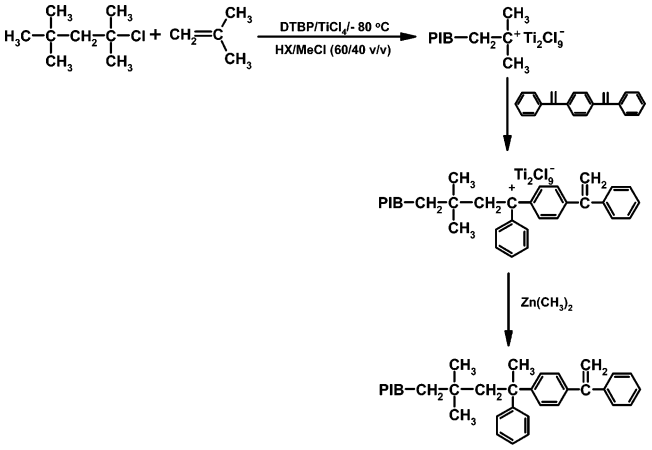

not possible to observe the PHEMA-*b*-PIB-*b*-PHEMA-coated stent surface using AFM. In general, the probe tip stuck to the surface, resulting in poor imaging, and, after hydration with the release medium, no phase morphology was visible.

Drug Release. Individual stents were analyzed for drug release in 1.5 mL of the release medium (PBS−Tween 20) at 37 °C. Previous studies have demonstrated that, because of the sampling frequency and sample size, sink conditions are maintained. In addition, the complete recovery of PTx has been demonstrated using mass balance evaluations after release. Elution of PTx was determined using HPLC analysis of the release medium using a proprietary method. At each time point, the release medium was analyzed for the level of PTx.

Results and Discussion

***ω*-DPE-Functionalized PIB (PIB-DPE).** Living PIB was prepared by the polymerization of IB with the TMPCl/$TiCl_4$ initiating system in the presence of DTBP as a proton trap in HX/MeCl 60/40 (v/v) at −80 °C. PIB-DPE was obtained by the reaction of living PIB with 2 equiv of PDDPE, followed by methylation of the resulting diphenyl carbenium ion with a large excess of $Zn(CH_3)_2$ ($Zn(CH_3)_2$]/[$TiCl_4$] = 5/1).[18,29] Figure 1 shows the ^{1}H NMR spectra of PIB and DPE end-functionalized PIB-DPE1 and PIB-DPE2. After the reaction of living PIB with PDDPE, peaks at 1.99 and 1.72 ppm assigned to the methylene and methyl protons at the PIB−Cl chain end disappeared, and new peaks at 7.42−7.20, 5.48−5.43, 3.07, and 2.52 ppm appeared due to the presence of the PDDPE moiety at the PIB chain end, as shown in Figure 1a,b. By using the ratio of M_n (GPC)/M_n (NMR), 95% and 108% DPE functionality was calculated for PIB-DPE1 and PIB-DPE2, respectively. Thus, capping is virtually quantitative. Figure 1c,d shows that, after methylation with $Zn(CH_3)_2$, a new peak at 1.82 ppm, assigned to the methyl proton at the PIB-DPE1 chain end, was observed; however, after 2 h, the peak at 3.07 ppm assigned to methoxy protons at the PIB-DPE chain end was still observed (Figure 1c) as a result of incomplete (94%) methylation.

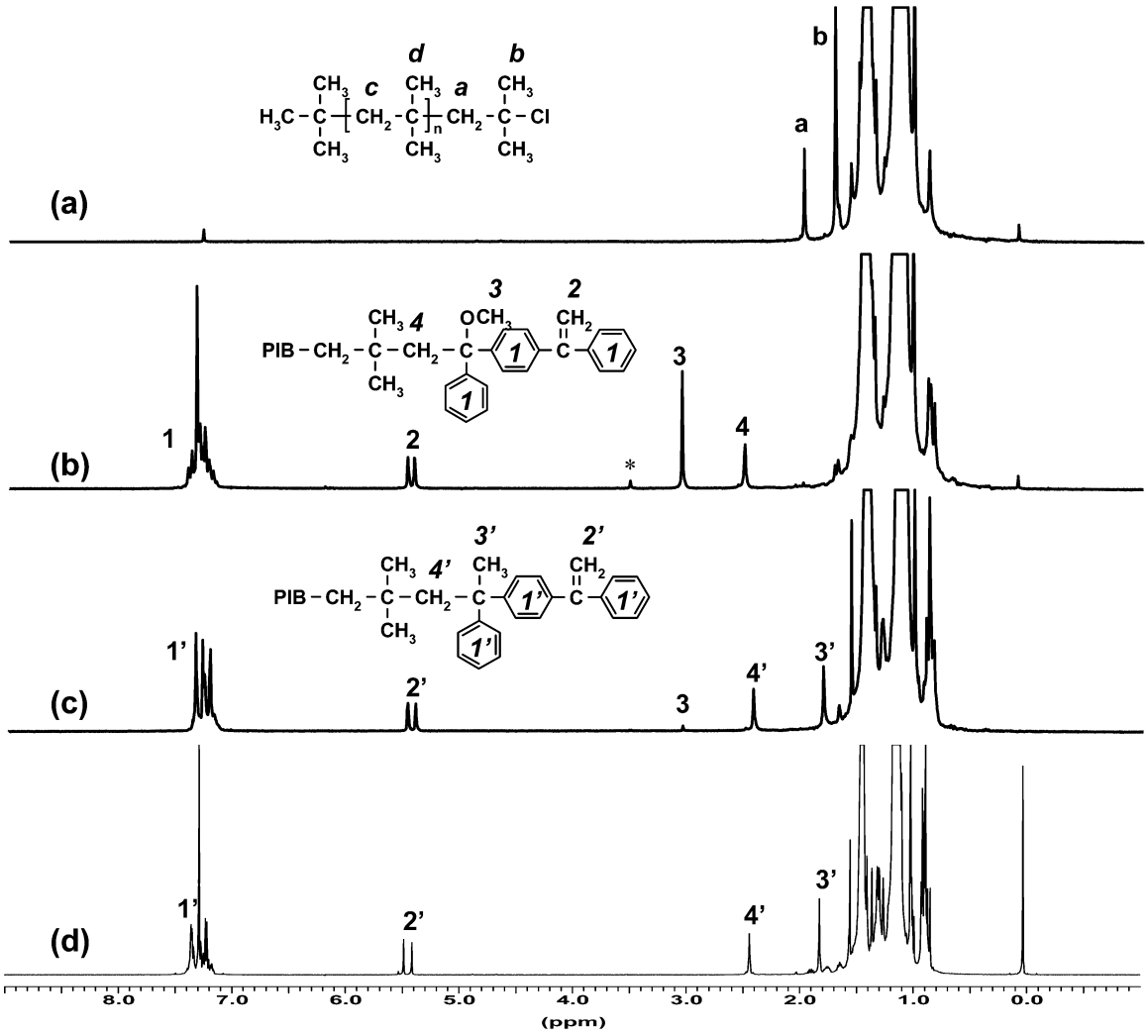

Figure 1. ^{1}H NMR spectra of (a) PIB, (b) PIB-DPE1 before, and (c) after methylation with $Zn(CH_3)_2$, and (d) 100% methylated PIB-DPE2.

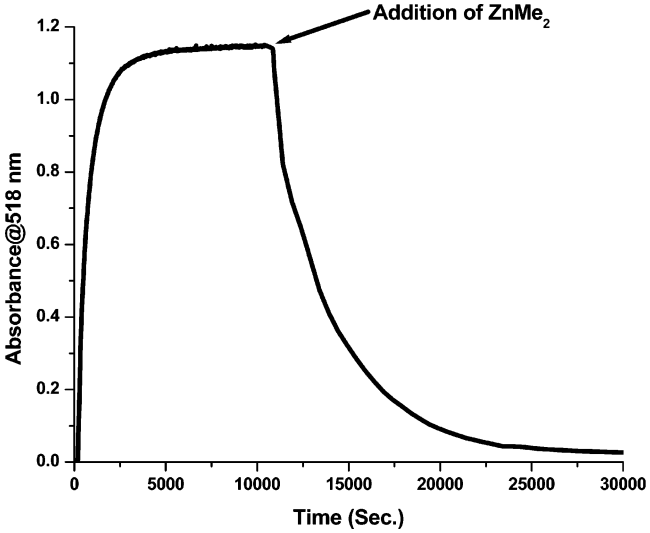

Figure 2. Plot of the absorbance at $\lambda = 518$ nm vs time for the PDDPE capping reaction and $ZnMe_2$ methylation of living PIB (M_n = 6100 g/mol; $M_w/M_n = 1.10$). Reaction conditions: [PIB] = 0.002 M; $[TiCl_4]$ = 0.036 M; [DTBP] = 0.004 M; [PDDPE] = 0.004 M; HX/MeCl = 60/40; −80 °C; $[Zn(CH_3)_2]/[TiCl_4]$ = 5/1.

Table 1. Characteristics of DPE-End-Functionalized PIB[a]

	PIB		PIB-DPE		DPE functionality	methylation yield
polymer	M_n	M_w/M_n	M_n	M_w/M_n	(%)[b]	(%)[c]
PIB-DPE1	4300	1.08	4900	1.05	95	94
PIB-DPE2	6100	1.10	6500	1.09	108	100
PIB-DPE3	6900	1.06	7200	1.08	110	100

[a] Functionalization conditions: [PDDPE]/[TMPCl] = 2/1; $[Zn(CH_3)_2]/[TiCl_4]$ = 5/1. [b] DPE functionality (%) = M_n (GPC)/M_n (NMR) × 100. [c] Determined by ^{1}H NMR.

In the synthesis of PIB-DPE2, in-situ UV−vis spectroscopy was employed to follow capping and methylation. According to Figure 2, capping is complete in 3 h; however, complete methylation, confirmed by the absence of resonances at 3.07 ppm in Figure 1d, required 5 h. The low reactivity of the cation arising from capping living PIB with PDDPE is attributed to higher resonance stabilization compared to that formed in the capping reaction of living PIB with DPE,[29] which could be methylated quantitatively in 2 h.

Table 1 presents the characteristics of PIB-DPE prepared using PDDPE and $Zn(CH_3)_2$. The fact that there is little difference in the M_w/M_n of PIB and that of PIB-DPE confirms the absence of a coupling reaction during the functionalization process.

PIB-*b*-PMMA. To avoid the termination of lithiated PIB formed in the reaction of PIB-DPE with *n*-BuLi, it is essential to ensure the complete absence of protic impurities in the PIB macromonomer. Since DPHLi cannot react with DPE because of steric hindrance, DPHLi could be utilized as a cleansing agent to remove protic impurities present in the polymer without reaction with PIB-DPE. For instance, Abetz et al. reported that protic impurities can be efficiently removed from a DPE-end-capped poly(1,2-butadiene) macromonomer by titration with a dilute solution of DPHLi.[30] Therefore, before lithiation of PIB-DPE with *n*-BuLi, dilute DPHLi solution, prepared by the reaction of PIB-DPE with excess *n*-BuLi in THF at −78 °C for 1 h, was added dropwise to the polymer solution until a yellowish color persisted. After DPHLi cleansing, two different lithiation procedures were employed to metalate PIB-DPE to form the anionic PIB macroinitiator (Scheme 2). In the first method, the polymer solution was cooled to −78 °C and 5−6 times excess *n*-BuLi was added. After 1 h, the polymer solution was warmed to 40 °C and kept at that temperature for 1 h to decompose unreacted *n*-BuLi.[31] Then, the polymer solution was cooled to −78 °C, and MMA was distilled into the reactor. In the second, simplified procedure, PIB-DPE was lithiated by 1.5 times excess *n*-BuLi at room temperature for 5−10 min. Upon the addition of *n*-BuLi, a blood-red color developed immediately, indicating the formation of PIB diphenyl carbanion. NMR (Figure 3) and UV−vis studies (not shown) showed that the lithiation of PIB-DPE is quantitative in 1 min. It is presumed that, during the remaining time, excess *n*-BuLi is destroyed by THF.

To determine the blocking efficiency, the GPC UV trace (254 nm) can be used because it detects the phenyl rings at the chain end of PIB-DPE1. As shown in Figure 4, the GPC UV trace of the block copolymer is bimodal. Since double bonds could not be detected in the ^{1}H NMR spectrum of homoPIB extracted with HX, metalation was quantitative. Therefore, the presence of homoPIB suggests that the PIB-DPE1 macroinitiator was deactivated during lithiation or MMA polymerization.

Table 2 shows the blocking efficiency of the block copolymers. Representative samples were extracted with HX, a selective solvent for homoPIB. The results agreed well with the calculated blocking efficiencies from the GPC UV traces. When the PIB macromonomer was not treated with DPHLi, the blocking efficiency was 56−70%, even though a large excess of *n*-BuLi ($[n\text{-BuLi}]_o/[\text{PIB-DPE}]_o$ = 10/1) was used for the lithiation of macromonomer. In contrast, when protic impurities were eliminated by titration with a small amount of DPHLi ($[\text{DPHLi}]_o/[\text{PIB-DPE}]_o$ = 0.1/1), the blocking efficiency increased up to 90%.

α,ω-DPE-Functionalized PIB (DPE-PIB-DPE). DPE-PIB-DPE with high molecular weight was prepared using *t*BuDiCumCl. The obtained difunctional macromonomer had narrow M_w/M_n (<1.11), indicating the absence of a coupling reaction.

PMMA-*b*-PIB-*b*-PMMA and PHEMA-*b*-PIB-*b*-PHEMA. The macromonomer was titrated with dilute DPHLi solution to remove impurities. The difunctional macroinitiator was obtained in the reaction of DPE-PIB-DPE with excess *n*-BuLi. Since high molecular weight PIB is insoluble in THF at −78 °C, THF/HX 70/30 (v/v) mixture solvents were used for the polymerization of MMA or TMSiOEMA.[15]

Scheme 2. Synthesis of PIB-*b*-PMA Copolymer Using PIB-DPE

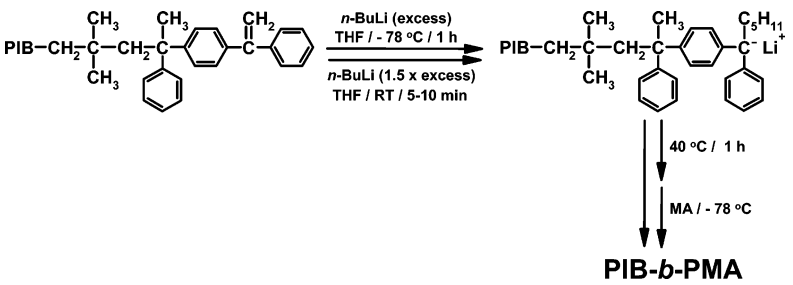

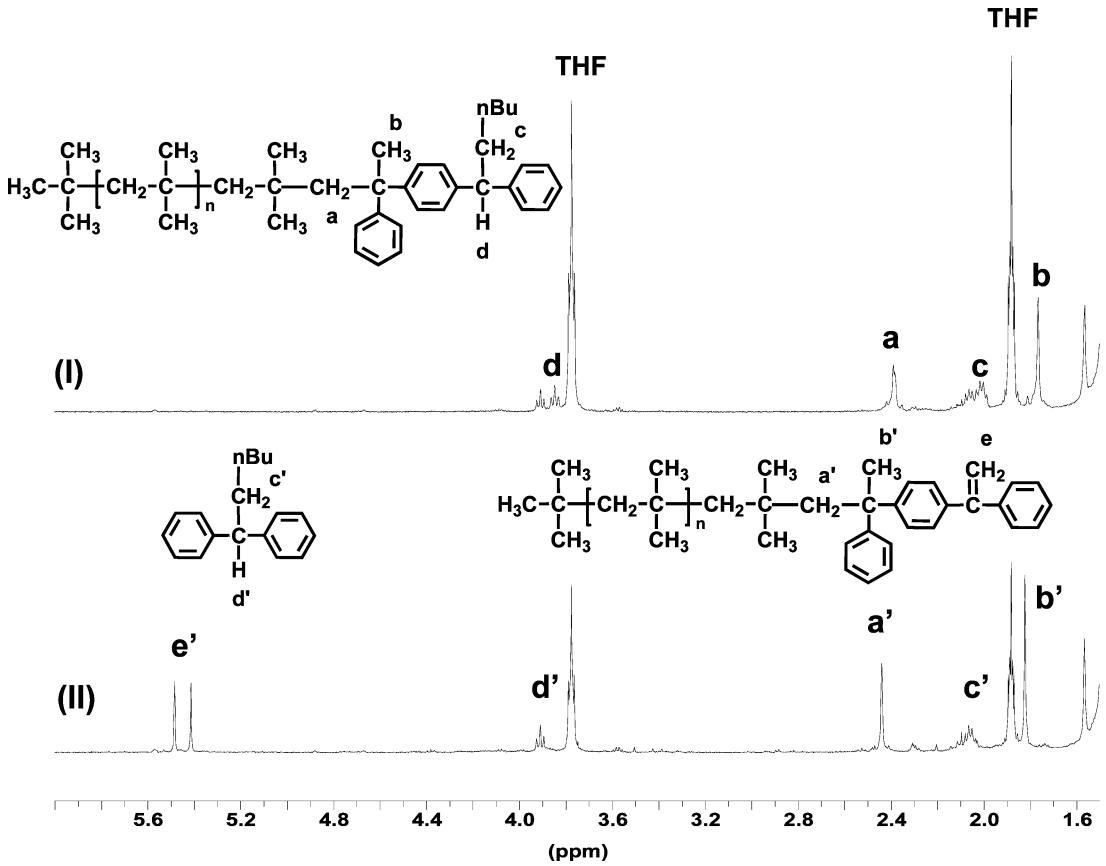

Figure 3. ^{1}H NMR spectrum of DPHLi-cleansed PIB-DPE2 (I) and the methanol-quenched PIB-DPE2 metalation product (II). (The singlet at 1.59 ppm is due to moisture.)

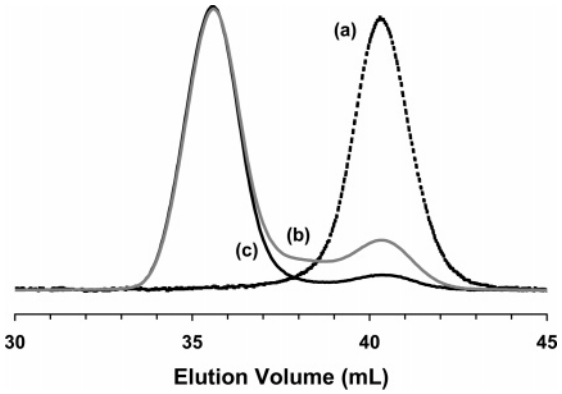

Figure 4. GPC traces of PIB-DPE1 ($M_n = 4900$; $M_w/M_n = 1.05$) and the AB5 copolymer: (a) RI trace of PIB-DPE1; (b) UV trace of AB5 copolymer; (c) RI trace of AB5 copolymer.

Table 2. M_n and Blocking Efficiencies (f) of PIB-*b*-PMMA Copolymers from PIB-DPE

	PIB-DPE						
polymer	M_n	M_w/M_n	$[n\text{-BuLi}]_o/[\text{PIB-DPE}]_o$	$[\text{DPHLi}]_o/[\text{PIB-DPE}]_o$	M_n (block)	M_w/M_n (block)	f (%)[a]
AB1	4900	1.08	10	0	23 300	1.14	56
AB2			10	0	37 200	1.10	61
AB3			10	0	29 900	1.09	70
AB4	4900	1.05	5	0.1	31 100	1.17	79
AB5			5	0.1	38 200	1.11	83
AB6	6500	1.09	1.5	0.1	31 100	1.17	82
AB7			5	0.1	38 200	1.11	80
AB8	7200	1.08	2	0.1	32 800	1.13	90

[a] Determined by the area of PIB precursor at GPC UV trace (254 nm).

The crude polymer was extracted with HX for 24 h to isolate the PIB precursor from the block copolymer. Figure 5 shows the GPC refractive index (RI) traces of PIB and the block copolymer (ABA1). After extraction, the M_w/M_n of ABA1 decreased from 1.16 to 1.13. According to ^{1}H NMR measurements, the extracted polymer was homoPIB. The M_w/M_n of block copolymer ABA4 did not change before and after purification as presented in Figure 6.

Table 3 shows the M_n, the M_w/M_n, the compositions, and the homoPIB contamination of the triblock copolymers. Thus, deactivated DPE-PIB-DPE could be reduced from 16% when macromonomer was not titrated with DPHLi to as low as 0.4−1% when PIB macromonomer was treated with DPHLi.

Differential Scanning Calorimetry. The DSC scans of PMMA-*b*-PIB-*b*-PMMA (ABA4) and PHEMA-*b*-PIB-*b*-PHEMA (ABA10) copolymers exhibit two T_g's, as shown in Figures 7 and 8, respectively. The T_g measured around −68 °C in both samples corresponds to PIB in both copolymers. The second measured T_g's at 122 and 95 °C correspond to the PMMA and PHEMA segments, respectively. The presence of two T_g's indicates the expected phase separation in both triblock copolymers.

Figures 7 and 8 also show DSC plots for PMMA-*b*-PIB-*b*-PMMA and PHEMA-*b*-PIB-*b*-PHEMA block copolymers after the addition of the therapeutic agent, PTx. Miscibility between the drug and a segment of a block copolymer would be demonstrated by a shift in the specific block glass transition toward the PTx T_g (150 °C). As shown in Figure 7, a shift in the T_g of the hard PMMA block of PMMA-*b*-PIB-*b*-PMMA to a temperature between the T_g of PTx and that of PMMA suggests miscibility between the PMMA and the PTx. In addition, the PMMA T_g increases with the amount of PTx added to the sample, and the plots show no indication of the PTx T_g.

The DSC plot generated for blends of PHEMA-*b*-PIB-*b*-PHEMA with 0, 10, and 25% PTx are shown in Figure 8. A

Table 3. M_n and IB wt % of Triblock Copolymers from a DPE-PIB-DPE Macromer

	macromer							deactivated macromer
polymer[a]	M_n	M_w/M_n	$[n\text{-BuLi}]_o/[\text{macromer}]_o$	$[\text{DPHLi}]_o/[\text{macromer}]_o$	M_n	M_w/M_n	IB[b] (wt %)	(%)[a]
ABA1[c]	55 400	1.11	6	0	133 000	1.13	45	16
ABA2[c]	55 400	1.11	6	0.1	100 600	1.12	57	11
ABA3[c]	56 800	1.04	6	0.2	109 400	1.14	57	6
ABA4[c]	56 800	1.04	6	0.2	83 400	1.30	67	1
ABA5[c]	64 000	1.14	6	0.1	87 000	1.15	74	4
ABA6[c]	65 300	1.12	5	0.2	92 600	1.12	70	1
ABA7[c]	54 200	1.16	1.5	0.1	81 200	1.18	68	5
ABA8[c]	65 000	1.12	1.5	0.1	99 700	1.10	64	0.4
ABA9[d]	53 300	1.08	6	0.3	86 700[e]		62	10
ABA10[d]	53 300	1.10	1.5	0.1	87 300[e]	1.18	67	5

[a] HX soluble part. [b] Determined by ^{1}H NMR. [c] PMMA-PIB−PMMA triblock copolymer. [d] PHEMA-PIB−PHEMA triblock copolymer. [e] Determined by GPC of the benzoylated derivative and ^{1}H NMR.

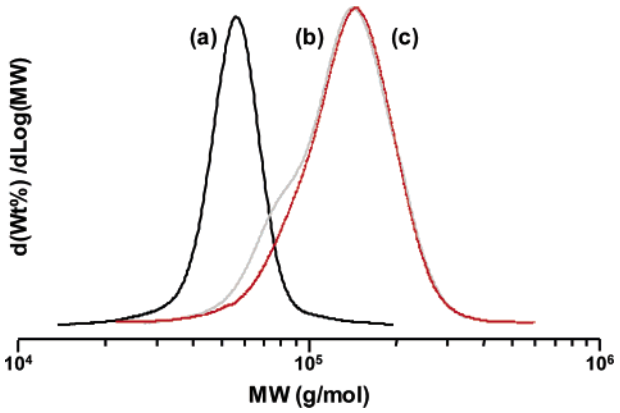

Figure 5. GPC RI traces of (a) DPE-PIB-DPE (M_n = 55 400, M_w/M_n = 1.11), (b) crude ABA1 copolymer (M_n = 121 800; M_w/M_n = 1.16), and (c) purified ABA1 copolymer (M_n = 130 500; M_w/M_n = 1.13).

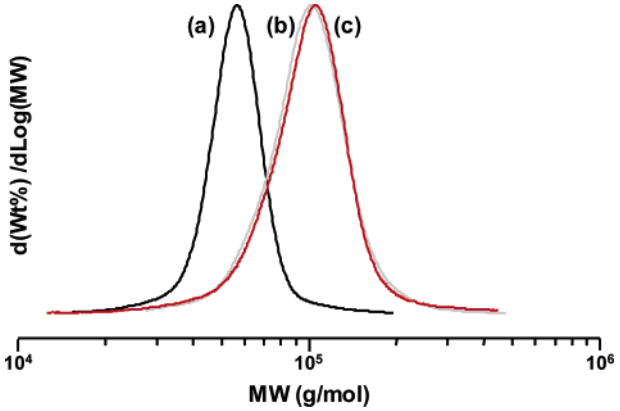

Figure 6. GPC RI traces of (a) DPE-PIB-DPE (M_n = 55 400; M_w/M_n = 1.11), (b) crude ABA2 copolymer (M_n = 94 700; M_w/M_n = 1.12), (c) purified ABA2 copolymer (M_n = 100 600; M_w/M_n = 1.12).

shift in the T_g of the PHEMA end-blocks toward the PTx T_g also suggests some degree of miscibility between the PHEMA and the PTx. Similar to the PMMA-*b*-PIB-*b*-PMMA and PTx results, the T_g of the HEMA block increases with the level of PTx in the blend, and no PTx T_g was detected.

Mechanical Properties. The tensile properties of representative PMMA-*b*-PIB-*b*-PMMA triblock copolymers were measured on compression-molded or solution-cast films, as shown by the stress−strain plots for ABA8 in Figure 9. As expected, based on previous reports,[32] films obtained by solution casting showed much better properties (16.5 MPa tensile strength and 560% ultimate elongation), indicating much better phase separation. Compression-molded samples exhibited a 10.5 MPa average tensile strength and 370% elongation at break. Since the tensile strength is very sensitive to the presence of diblock copolymer, the excellent tensile strength suggests that the diblock contamination, if any, is very low.

SEM of Stent Coatings. SEM images of representative coated stents are shown in Figure 10. The coating formulation shown in Figure 10 is 25% PTx/75% PMMA-*b*-PIB-*b*-PMMA (ABA2). After application of the coating solution to the stent using a proprietary technique, the coated stents were dried to remove solvents. The total coverage (drug and polymer) was adjusted so all stents contained the same total amount of PTx. A smooth conformal coating is produced, which completely covers the stent struts without filling in the interstitial spaces between struts. During use and deployment, the stent is expanded by an angioplasty balloon until it presses against the blood vessel wall. The polymeric-based coating undergoes a significant degree of rapid expansion in the struts joints (up to 300% elongation for some stent platforms). In addition, the coating is also subject to a small level of compression on the opposite side of the strut. It is critical that the polymeric carrier exhibit elastomeric properties that allow the elongation and compression of the material to occur without cracking or deformation of the coating as shown.

AFM of Stent Coatings. AFM phase images of the surface of stents coated with the SIBS copolymer and formulations containing 91.2% SIBS/8.8% PTx are shown in Figure 11. The image in Figure 11a shows the expected phase-separated morphology that results after coating and drying the block copolymer. After incorporation of the PTx into the coating, a third discrete dispersed phase is visible within the SIBS two-phase morphology, as seen in Figure 11b. Examination of the drug-loaded stent surface after 24 h of exposure to the release media, as shown in Figure 11c, exhibits the voids that remain in the surface of the stent after elution of the drug. Interestingly, the two-phase morphology of the copolymer remains undisturbed after elution of PTx.

Images of the PMMA-*b*-PIB-*b*-PMMA (ABA6) copolymer and 75% PMMA-*b*-PIB-*b*-PMMA (ABA6) copolymer/25% PTx formulations are shown in Figure 12. Similar to images shown for the SIBS copolymer, the two-phase morphology of the block copolymer is clearly visible. However, the dispersed drug is not visible in the formulations containing 25% PTx, despite the increase in the drug loading relative to the SIBS formulations.

Figure 13 shows both the phase and topography images taken from 75% PMMA-*b*-PIB-*b*-PMMA (ABA6) copolymer/25% PTx coated stents after immediate and 24 h exposure to release medium. The two-phase morphology is visible after imaging

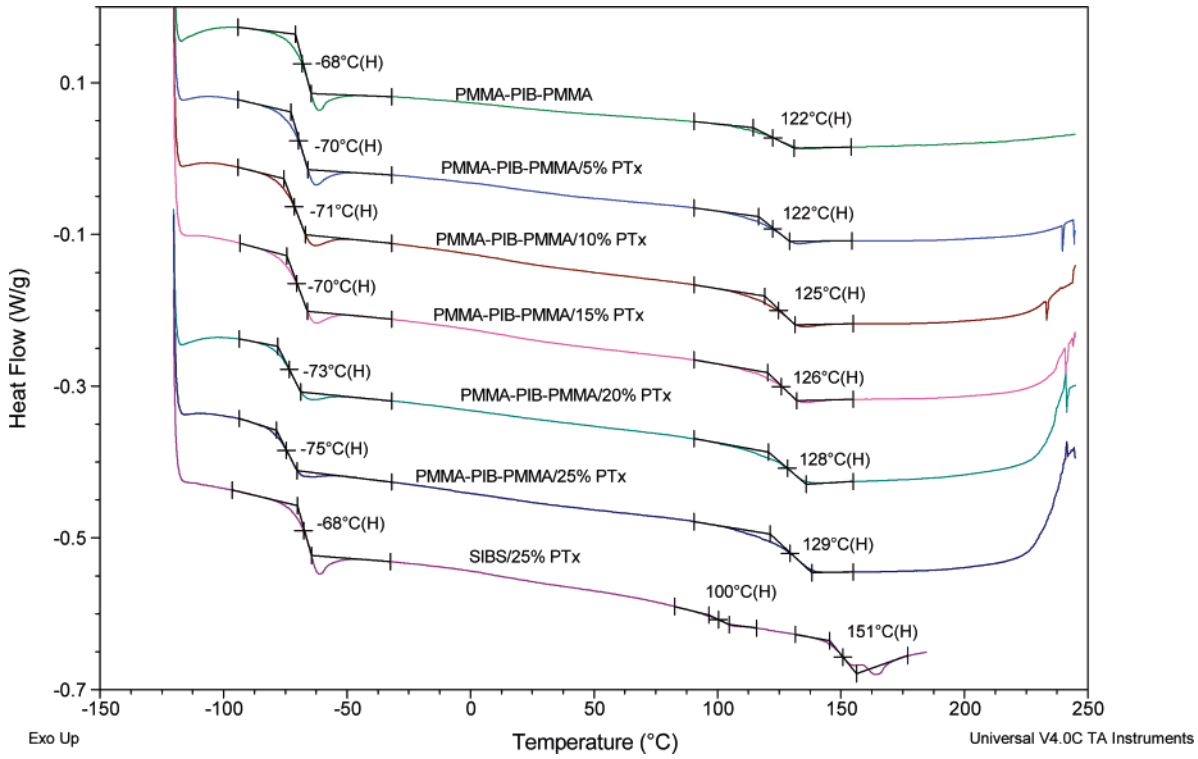

Figure 7. DSC thermograms of PMMA-*b*-PIB-*b*-PMMA films containing 0, 5, 10, 15, 20, and 25% PTx.

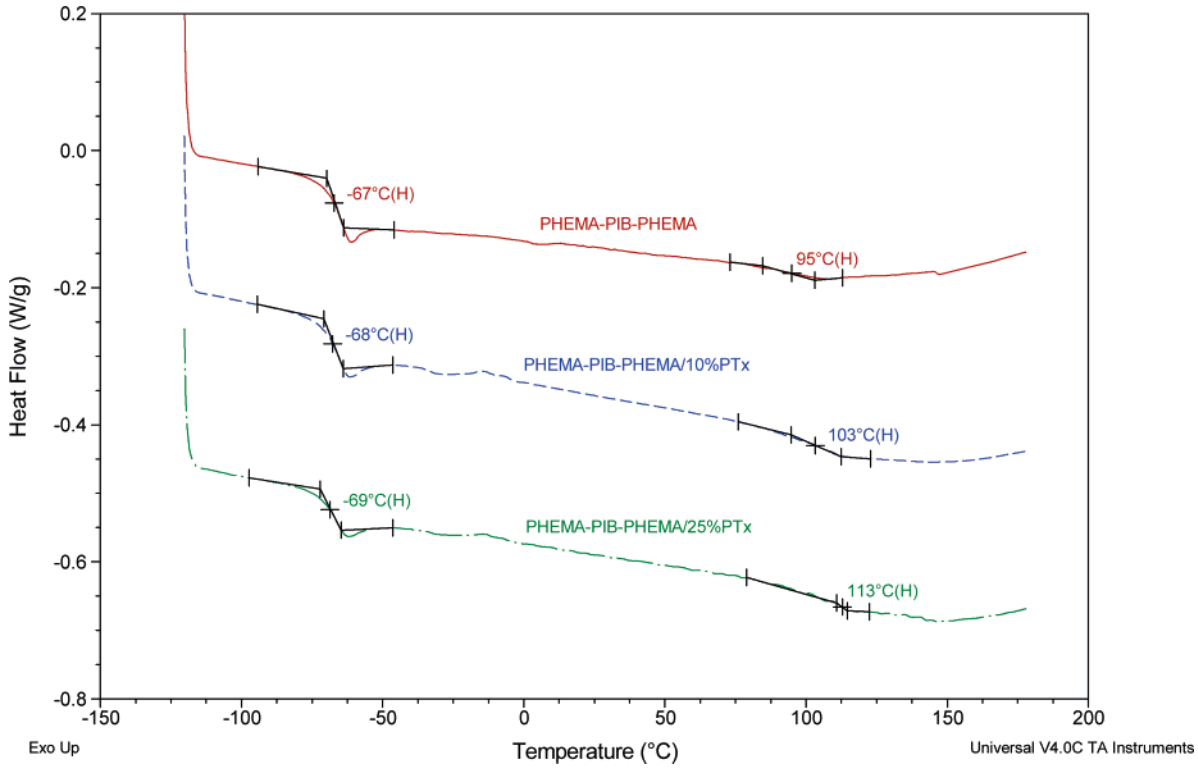

Figure 8. DSC thermograms of PHEMA-*b*-PIB-*b*-PHEMA films containing 0, 10, and 25% PTx.

under the release medium for both formulations. The surface of the coated stent after immediate exposure to fluid appears to be similar to the dry imaged surface, although there is some loss of resolution due to imaging under a fluid. However, it appears that voids are visible in the images of the stents coated with 75% PMMA-*b*-PIB-*b*-PMMA copolymer/25% PTx. Close examination of the topography image shows that these may not be voids, but rather raised regions that surround a very small void. These appear to be an eruption on the surface as the embedded PTx is released from subsurface regions in the coating.

Drug Release. Figure 14 shows the cumulative % of loaded PTx released from stents coated with 8.8% PTx and 91.1% of either PMMA-*b*-PIB-*b*-PMMA (ABA3), PHEMA-*b*-PIB-*b*-PHEMA (ABA9), or SIBS. In addition, Table 4 tabulates the amount of PTx released within the initial 1−2 days of testing,

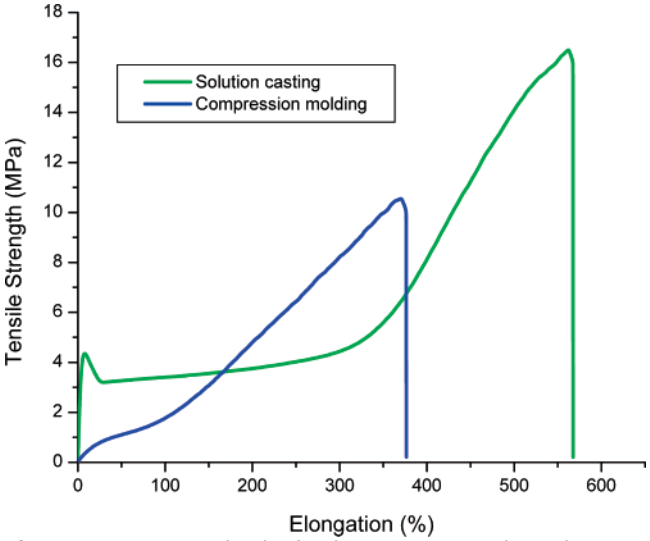

Figure 9. Stress−strain plot for the ABA8 PMMA-*b*-PIB-*b*-PMMA triblock copolymer.

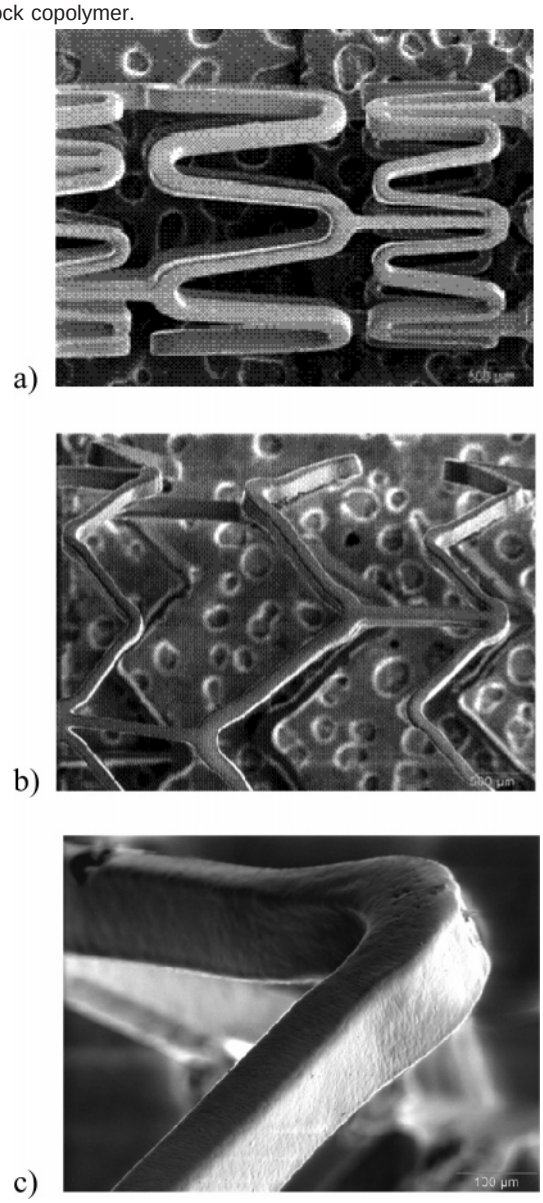

Figure 10. SEM images of coronary stents coated with 25% PTx and 75% PMMA-*b*-PIB-*b*-PMMA (ABA2): (a) SEM micrograph of an unexpanded coated stent at 40×; (b) SEM micrograph of an expanded coated stent at 40×; (c) SEM micrograph of an expanded coated stent at 200×.

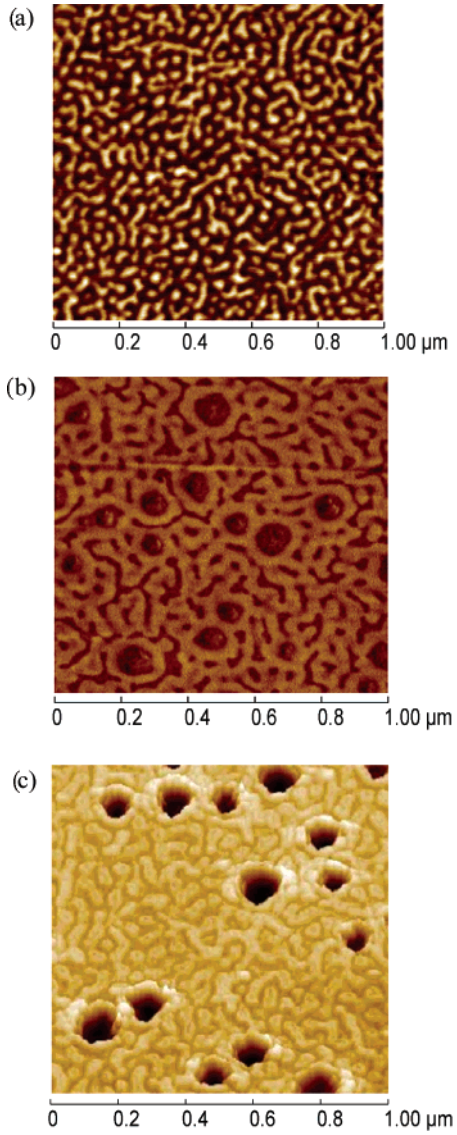

Figure 11. High-resolution 1 μm phase AFM image of the surface of a stent coated with (a) SIBS copolymer imaged in air, (b) a blend containing 75% SIBS/25% PTx imaged in air, and (c) a blend containing 75% SIBS/25% PTx imaged after 24 h of incubation in the release media showing holes remaining after the elution of PTx.

and the subsequent rate of PTx released over the remainder of the test interval. The release from both the PHEMA-*b*-PIB-*b*-PHEMA and SIBS copolymers is characterized by an initial burst of PTx that occurs during the initial 1−2 days of testing, followed by a slower sustained release. Both the burst and rate of PTx release from stent coatings formulated with PHEMA-*b*-PIB-*b*-PHEMA are significantly greater than the amount released from those with SIBS. Although the total release of PTx from stents coated with PMMA-*b*-PIB-*b*-PMMA appears to be similar to the SIBS copolymer, the release does not show an initial burst release of PTx. Instead, the release profile shows a slow, constant release of PTx over the time period of testing. It is postulated that the increase in the hydrophilicity of the PHEMA-*b*-PIB-*b*-PHEMA copolymer allows the aqueous release medium to rapidly diffuse into the coating to permit more effective dissolution and extraction from the surface and subsurface of the polymer coating, resulting in a rapid release of PTx.

Changes in the release kinetics with the copolymer formulation may be more apparent at higher loadings of PTx. Figure 15 shows the PTx released from stent coatings containing 25%

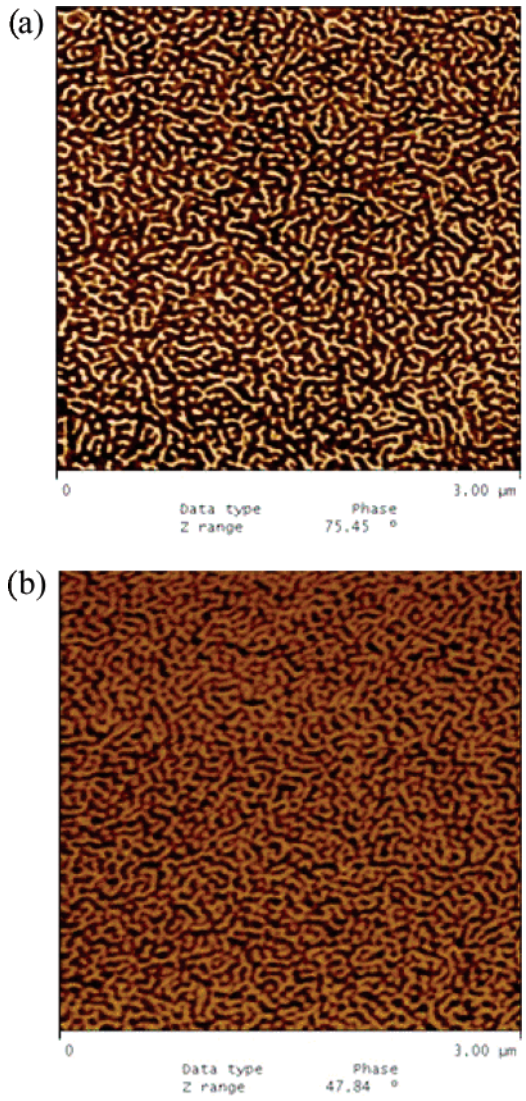

Figure 12. High-resolution 3 μm phase AFM image of the surface of a stent coated with (a) 100% PMMA-*b*-PIB-*b*-PMMA (ABA6) copolymer imaged in fluid and (b) 75% PMMA-PIB-PMMA copolymer (ABA6)/25% PTx imaged in air.

PTx blended with 75% of either PMMA-*b*-PIB-*b*-PMMA (ABA2), PHEMA-*b*-PIB-*b*-PHEMA (ABA9), or SIBS. The PTx release profile from coatings with both PHEMA-*b*-PIB-*b*-PHEMA and SIBS appear to be similar to those measured from coatings formulated with 8.8% PTx. Interestingly, approximately 36% of the loaded PTx burst from the PHEMA-*b*-PIB-*b*-PHEMA coatings, independent of the drug formulation. However, the measured rate of PTx eluting after the initial burst release increased from approximately 1.6 to 2.0 cumulative %PTx/day as the loading increased from 8.8 to 25%.

The slow sustained release of PTx from stents coated with PMMA-*b*-PIB-*b*-PMMA is more evident with 25% PTx formulated in the coating. It is hypothesized that this slow sustained release profile is due to potential interactions between PTx and PMMA end-blocks that may control the rate of diffusion of PTx from the coating. Miscibility between PTx and the hard PMMA end-blocks of the copolymer were detected by shifts in the T_g of the PMMA blocks after the addition of PTx, as measured using DSC and shown in Figure 7. In contrast, according to a recent report, PTx is miscible with the poly(butylacrylate) (PBA) middle block and immiscible with the PMMA hard block in PMMA-*b*-PBA-*b*-PMMA,[33] indicating the importance of the chemical nature of both blocks in determining the distribution of PTx.

In summary, the burst release from the PHEMA-*b*-PIB-*b*-PHEMA copolymer supports the theory that the polymer hydrophilicity, resulting in increased swelling of the polymer matrix, plays a role in the release behavior. Similar release

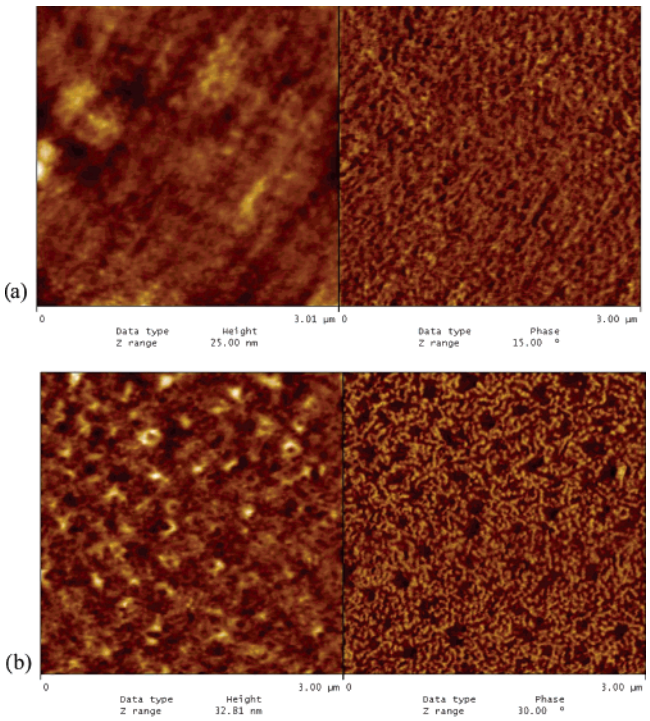

Figure 13. High-resolution tapping-mode 3 μm AFM image taken of 75% PMMA-*b*-PIB-*b*-PMMA (ABA6)/25% PTx coated stent surfaces after (a) 0 min and (b) 24 h exposure to release medium showing the topography (left) and phase (right) data.

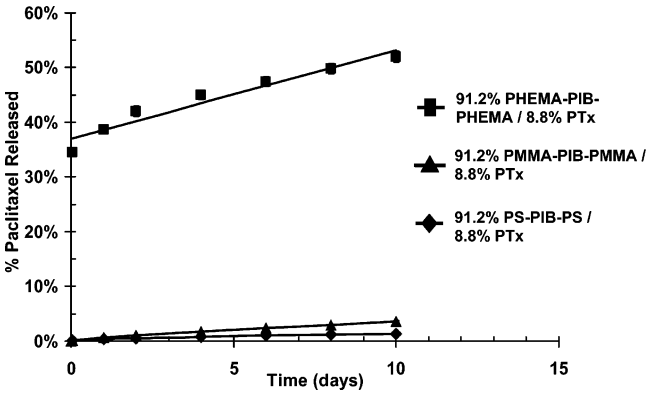

Figure 14. Release of PTx from coronary stents coated with formulations containing 8.8% PTx and 91.2% of either PMMA-*b*-PIB-*b*-PMMA (ABA3), PHEMA-*b*-PIB-*b*-PHEMA (ABA9), or PS-*b*-PIB-*b*-PS. Error bars were used to show the spread in the data at each time point, but they are small and hidden by the symbols.

Table 4. Cumulative % of Loaded PTx Released during the Initial 24 h of In Vitro Release Testing, and the Subsequent Rate of PTx Release after the Initial 24−48 h of Testing

	8.8% PTx formulations		25% PTx formulations	
copolymer	burst (%PTx)	rate PTx release (%PTx/day)	burst (%PTx)	rate PTx release (%PTx/day)
PS-*b*-PIB-*b*-PS	0.4	0.1	2.5	0.1
PMMA-*b*-PIB-*b*-PMMA	0.2	.36	0	2.1
HEMA-*b*-PIB-*b*-HEMA	37	1.6	36	2.0

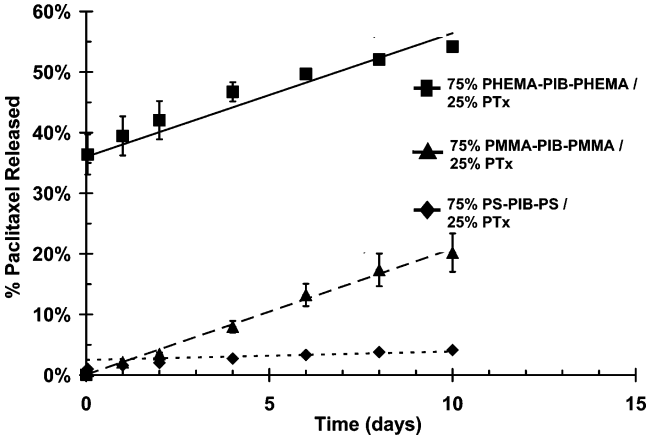

Figure 15. Release of PTx from coronary stents coated with formulations containing 25% PTx and 75% of either PMMA-*b*-PIB-*b*-PMMA (ABA 3), PHEMA-*b*-PIB-*b*-PHEMA (ABA9), or PS-*b*-PIB-*b*-PS.

profiles were measured previously for PIB-based block copolymers with hydrophilic end blocks.[10] Other factors, such as the solubility of the drug in the polymer matrix, also play a role in determining the PTx release profile, as demonstrated by correlating the miscibility determined by DSC analysis of PMMA-*b*-PIB-*b*-PMMA and PTx blends.

Conclusions

PIB−PMMA diblock and triblock copolymers were successfully synthesized by the combination of cationic and anionic polymerization. Metalation of DPE-end-functionalized PIB prepared from the reaction of living PIB with PDDPE was achieved by simple reaction with *n*-BuLi, and the yield was quantitative. The resulting macroanion could efficiently initiate the polymerization of MMA. This methodology is suggested to be the most convenient for the synthesis of PIB-based block copolymers. Cleansing of the PIB-DPE solution with DPHLi eliminated the need for a critical purification of macromonomer, which further simplified the synthesis of block copolymers by avoiding the use of a large excess of *n*-BuLi for the formation of the macroinitiator and the warming−cooling steps for the removal of unreacted *n*-BuLi.

The resulting PMMA-*b*-PIB-*b*-PMMA and PHEMA-*b*-PIB-*b*-PHEMA copolymers exhibited physical properties suited for stent-coating applications and were successfully formulated with PTx and coated on coronary stents. DSC evaluations of PMMA-*b*-PIB-*b*-PMMA/PTx blends showed miscibility between the PMMA end-blocks and PTx, resulting in a sustained first-order release of PTx from coated stents. However, the hydrophilic nature of PHEMA resulted in a burst release of PTx from the PHEMA-*b*-PIB-*b*-PHEMA/PTx-coated stents. AFM analysis of the coated stent surface shows the expected phase morphology of the block copolymers and voids remaining after elution of PTx.

References and Notes

(1) Stone, G. W.; Ellis, S. G.; Cox, D. A.; Hermiller, J.; O'Shaughnessy, C.; Mann, J. T.; Turco, M.; Caputo, R.; Bergin, P.; Greenberg, J.; Popma, J. J.; Russell, M. E. *N. Engl. J. Med.* **2004**, *350*, 221.
(2) Colombo, A.; Drzewiecki, J.; Banning, A.; Grube, E.; Hauptmann, K.; Silber, S.; Dudek, E.; Fort, S.; Schiele, F.; Zmudka, K.; Guagliumi, G.; Russell, M. E. *Circulation* **2003**, *108*, 788.
(3) Sousa, J. E.; Costa, M. A.; Abizaid, A. C.; Rensing, B. J.; Abizaid, A. S.; Tanajura, L. F.; Kozuma, K.; Van Langenhove, G.; Sousa, A. G. M. R.; Falotico, R.; Jaeger, J.; Popma, J. J.; Serruys, P. W. *Circulation* **2001**, *104*, 2007.
(4) Regar, E.; Serruys, P. W.; Bode, C.; Holubarsch, C.; Guermonprez, J. L.; Wijns, W.; Bartorelli, A.; Constantini, C.; Degertekin, M.; Tanabe, K.; Disco, C.; Wuelfert, E.; Morice, M. C. *Circulation* **2002**, *106*, 1949.
(5) Lemos, P. A.; Saia, F.; Ligthart, J. M. R.; Arampatzis, C. A.; Sianos, G.; Tanabe, K.; Hoye, A.; Degertekin, M.; Daemen, J.; McFadden, E.; Hofma, S.; Smits, P. C.; de Feyter, P.; van der Giessen, W. J.; van Damberg, R. T.; Serruys, P. W. *Circulation* **2003**, *108*, 257.
(6) Sousa, J. E.; Serruys, P. W.; Costa, M. A. *Circulation* **2003**, *107*, 2274.
(7) Sousa, J. E.; Serruys, P. W.; Costa, M. A. *Circulation* **2003**, *107*, 2383.
(8) Ranade, S. V.; Miller, K. M.; Richard, R. E.; Chan, K.; Allen, M. J.; Helmus, M. N. *J. Biomed. Mater. Res.* **2004**, *71A*, 625.
(9) Zhou, Y.; Faust, R.; Richard, R.; Schwarz, M. *Macromolecules* **2005**, *38*, 8183.
(10) Sipos, L.; Som, A.; Faust, R.; Richard, R.; Schwarz, M.; Ranade, S.; Boden, M.; Chan, K. *Biomacromolecules* **2005**, *6*, 2570.
(11) Ranade, S.; Richard, R.; Helmus, M. *Acta Biomater.* **2005**, *1*, 137.
(12) Lewis, G. *J. Biomed. Mater. Res.* **1998**, *38*, 155.
(13) Nicolson, P. C.; Vogt, J. *Biomaterials* **2001**, *22*, 3273.
(14) Feldthusen, J.; Ivan, B.; Muller, A. H. E. *Macromolecules* **1997**, *30*, 6989.
(15) Feldthusen, J.; Ivan, B.; Muller, A. H. E. *Macromolecules* **1998**, *31*, 578.
(16) Feldthusen, J.; Ivan, B.; Muller, A. H. E.; Kops, *J. Macromol. Symp.* **1996**, *107*, 189.
(17) Martinez-Castro, N.; Lanzendolfer, M. G.; Muller, A. H. E.; Cho, J. C.; Acar, M. H.; Faust, R. *Macromolecules* **2003**, *36*, 6985.
(18) Bae, Y. C.; Faust, R. *Macromolecules* **1998**, *31*, 9379.
(19) Bae, Y. C.; Fodor, Zs.; Faust, R. *Macromolecules* **1997**, *30*, 198.
(20) Hadjikyriacou, S.; Faust, R. *Macromolecules* **1996**, *29*, 5261.
(21) Gyor, M.; Wang, H. C.; Faust, R. *J. Macromol. Sci., Pure Appl. Chem.* **1992**, *A29*, 639.
(22) Tung, L. H.; Lo, G. Y.-S. US Patent 4,182,818, 1980.
(23) Allen, R. D.; Long, T. E.; McGrath, J. E. *Polym. Bull. (Berlin)* **1986**, *15*, 127.
(24) Mori, H.; Wakisaka, O.; Hirao, A.; Nakahama, S. *Macromol. Chem. Phys.* **1994**, *195*, 3213.
(25) Fodor, Zs.; Faust, R. *J. Macromol. Sci., Pure Appl. Chem.* **1994**, *A31*, 1985.
(26) Li, D.; Faust, R. *Macromolecules* **1995**, *28*, 1383.
(27) Hadjikyriacou, S.; Faust, R. *Macromolecules* **1995**, *28*, 7893.
(28) Hirao, A.; Kato, H.; Yahoguchi, K.; Nakahama, S. *Macromolecules* **1986**, *19*, 1294.
(29) Bae, Y. C.; Kim, I.; Faust, R. *Polym. Bull. (Berlin)* **2000**, *44*, 453.
(30) Huckstadt, H.; Gopfert, A.; Abetz, V. *Macromol. Chem. Phys.* **2000**, *201*, 296.
(31) Rembaum, A.; Siao, S.; Indicator, N. *J. Polym. Sci.* **1962**, *56*, S17.
(32) Quirk, R. P.; Morton, M. In *Thermoplastic Elastomers*; Holden, G., Legge, N. R., Quirk, R., Schoeder, H. E., Eds.; Hanser/Gardner: Cincinnati, OH, 1996; p 79.
(33) Richard, R. E.; Schwarz, M.; Ranade, S.; Chan, A. K.; Matyjaszewski, K.; Sumerlin, B. *Biomacromolecules* **2005**, *6*, 3410.

BM0604496